

# **Rail Crack Monitoring Using Fiber Optic Based Ultrasonic Guided Wave Detection Technology**

---

JUNFANG WANG, MAODAN YUAN and YI-QING NI

## **ABSTRACT**

Rail health conditions are among the top concerns in the area of train safety. In this study, a fiber optic monitoring system is developed to achieve ultrasonic guided wave based rail crack detection. Although fiber Bragg grating (FBG) sensor is a well-known suitable candidate for long-distance monitoring of rail, the sampling speed of commercially available optic spectrum analyzers limits their application to ultrasonic wave detection. A high-speed FBG interferometric interrogation module is developed, which constitutes the rail monitoring system in conjunction with an active wave generation module and a sensing network. To find appropriate excitation frequency and FBG dimension for ultrasonic guided wave generation and reception, dispersion analysis of rail, a waveguide with complex cross-section, is conducted to guide subsequent design of damage detection experiment. The system and the crack detection technique are then implemented on a long full-scale rail segment, by deploying PZT (lead zirconate titanate) actuator and FBG sensor in pitch-catch and pulse-echo configurations. Artificial cracks in different lengths are introduced to the rail. Frequency-domain analysis of the rail responses is used to identify the damage-induced discrimination after direct observation of time-domain signals. Power spectral density analysis of the purified signals, assisted by discrete wavelet filtering, leads to the graphic presentation of rail integrity.

## **INTRODUCTION**

As subjected to very high and frequent service loads, rail suffers from fatigue and excessive tensile stress, which make it prone to cracking. Undetected crack may lead to the breakdown of rail signaling system, and further development of the crack may cause catastrophic consequences such as derailment. Given such significance, its health condition is thus among the top concerns for train safety.

Over past decades, both non-destructive evaluation (NDE) and structural health monitoring (SHM) techniques have been advocated as preventative measures against

---

Junfang Wang, Maodan Yuan, and Yi-Qing Ni, Hong Kong Branch of National Rail Transit Electrification and Automation Engineering Technology Research Center, The Hong-Kong Polytechnic University, Kowloon, Hong Kong.

the immense life and monetary loss resulting from rail damage. The most common NDE techniques used for detecting rail defects are magnetic induction tests [1] and ultrasonic tests [2]. Although playing a significant role in perceiving structural anomalies, most of them can only be maneuvered offline for regular rail inspection at a periodical interval. In this regard, Ultrasonic Guided Wave (UGW) based detection techniques, benefiting from the superb characteristics of guided wave, including convenience in actuation, high sensitivity to local discontinuities, low attenuation, and strong penetration [3], can potentially circumvent the aforementioned insufficiency, realize continuous monitoring without the interruption of train operation, and meanwhile offer long-range interrogation capability [4-5].

Both insulated piezoelectric sensors and FBG sensors are suitable candidates permanently deployed on rail tracks for UGW based online monitoring. Although piezoelectric transducers are extensively adopted because of their dual roles of activating and receiving ultrasonic waves, large-range monitoring of a rail track by densely distributed piezoelectric transducers becomes infeasible. Electric power is required for each of the piezoelectric transducers, but the power supply is usually unavailable along a rail line. In contrast, FBG sensors are characterized by excellent multi-functionality and multiplexing capabilities. It combines several data streams in separate time/frequency ranges from the same or different functions of FBG sensors into one optic fiber, and thus avoids the disadvantage of piezoelectric sensor and meanwhile facilitates the long-range monitoring of rail. Other characteristics of FBG sensors, such as small size, light weight, immunity to electromagnetic interference, and corrosion resistance, also make them desirable in rail condition monitoring. Despite that, its application to the UGW based long-range monitoring of rail is rarely reported. The major challenge of applying FBG sensors to guided wave measurement is capturing local dynamic micro-strains with a low amplitude but an ultrasonic frequency. Commercially available FBG optic spectrum analyzers (interrogators) generally have a nominal sampling speed of only several kilo-Hertz. It is almost impossible for them to acquire such high-speed strain change in micro-strain level and meanwhile guarantee low noise level.

In this investigation, an interrogation system enabling the detection of FBG wavelength shift down to a few deci-picometers (pm) at a sampling rate of 1 MHz is developed. A PZT-FBG hybrid scheme is deployed herein for guided wave activation and reception. It is implemented on a full-scale rail segment, by deploying two PZT actuators and one FBG sensor in pitch-catch and pulse-echo configurations. Such a scheme intends to fully exploit the merits of PZT transducers and FBG sensors while circumvents the disadvantages in the distributive deployment of PZT transducers. The following sections in this paper report on the rail defect detection by using the hybrid configuration and the developed interrogator prototype.

## **EXPERIMENTATION**

### **Experimental system**

Successful generation and acquisition of guided waves are key prerequisites for damage detection. A full-scale rail test bed has been established, in which the 10 m rail segment is equipped with a wave generation unit, an interrogator, and transducers

for wave actuation and reception (Figures 1-2). The test bed is shown in Figures 1-2, with Figure 2 illustrating the optic/electric circulation between the devices. This system, designed to accommodate ultrasonic guided wave detection with the use of FBG sensors, features the following electric and optic components. The excitation is a tone burst of which the amplitude, number of cycles, and frequency are controllable via the interface of wave generation unit. It is emitted from the PC-controlled wave generation unit in a manner of periodic scans and then transmitted to a PZT actuator after being amplified as high energy driving pulses. The initial version of this FBG interrogation module has a sampling rate of 1 MHz and a noise level of -130 dB nm/ $\sqrt{\text{Hz}}$ . The latter parameter means it can detect FBG wavelength shift down to no more than 0.3 pm. Although the devised system supports only one FBG sensor at that stage, the use of wave-division multiplexing technology potentially enables the distributed monitoring of rail condition with FBG sensors.

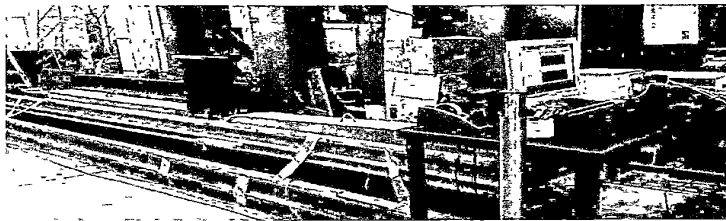


Figure 1 Test bed.

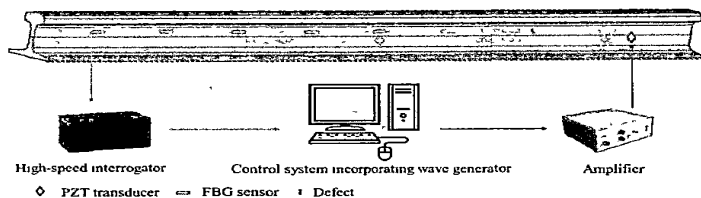


Figure 2 Schematic of the PZT-FBG experimental system

Transducers are deployed in an architecture that two PZT actuators are located at both sides of one FBG sensor (Figure 3). While facilitating both pulse-echo (damage is outside actuator-sensor path) and pitch-catch (damage is between an actuator and a sensor) configurations, it also provides certain redundancy. For laboratory tests reported in this study, the locations of the actuator, sensor, and crack are 1 m, 2 m, and 1.5 m respectively in pitch-catch configuration; their locations are 3 m, 2 m, and 1.5 m respectively in pulse-echo configuration. When a high-speed interrogator capable of multiplexing to tens or hundreds of FBGs is available, a transducer placement scheme based on even distribution can be adopted, in which every two adjacent transducers are spaced at a fixed interval along the longitudinal direction of rail. For the field application of rail defect identification, it is usually time-consuming and sometimes

infeasible to design an optimal sensor placement architecture. An evenly distributed placement method tends to achieve an effortless and general solution to practical implementation.

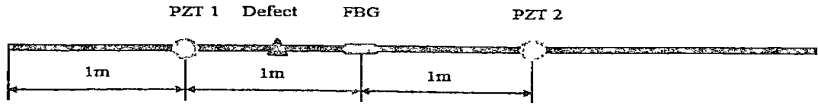


Figure 3. Actuator-sensor placement

### Wave dispersion and attenuation analysis for experiment design

As the prototyped interrogator can support limited number of FBG sensor, the dispersion and wave attenuation analyses were conducted by using PZT transducers. To improve measurement confidence, seven PZT transducers are distributed along the rail at 1, 2, 4, 5, 6, 8, and 9 m, with the transducer at 1 m as an actuator and others as sensors. The dispersion characteristic was obtained by dividing the distance between actuation and perception positions by the time difference between excitation and received signals and then averaging all the quotients. By altering the excitation frequency, the dispersion curve (i.e. wave velocity against frequency) is yielded (Figure 4). In the low-frequency range, the wave velocity increases with frequency, indicating remarkable dispersion characteristic. For the excitation frequency higher than 70 kHz, group velocity becomes almost constant with little fluctuation, thus almost non-dispersive. We chose 90 kHz and 100 kHz as the center frequencies of excitation tone bursts in laboratory tests. FBG sensors with their gratings customized to cover 20-125 kHz and their coating and re-coating conducive to the good coupling with ultrasonic wave were selected accordingly. In addition, to evaluate the wave attenuation property, the amplitudes of first-arrival wave packages at different measurement points are depicted in Figure 5. When propagating from 4 m to 9 m, it is seen that the amplitudes of guided wave have very slight attenuation.

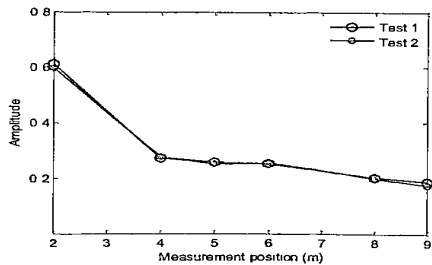
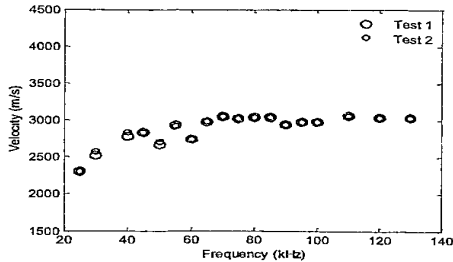


Figure 4 Dispersion curve – velocity against frequency      Figure 5 Insignificant attenuation of guided wave

## DATA ANALYSIS AND FEATURE EXTRACTION

### Time-domain analysis

The excitation signal is tone burst composed of ten cycles of sinusoidal wave and generated at a repetition rate of 10 per second. The sampling frequency is 1 MHz, and the duration for data acquisition is 5 seconds. The typical responses induced by one tone-burst excitation are depicted in Figures 6-7. Two artificial cracks, with 10 and 23 mm in length respectively, were introduced at the location of 1.5 m (Figure 3 (b)) by a sharp abrasive cutting roller. Affected by the diameter of roller blade, the smaller crack of 10 mm has a shallow extension at its two sides, and thus the total length becomes approximately 15 mm; likewise, the bigger crack of 23 mm in length has an extension of 1-2 mm. Differences between intact and damaged situations can be observed in these responses though they are not evident. By making a comparison between Figures 6 and 7, it is found that the pulse-echo configuration exhibits higher sensitivity to damage than the pitch-catch configuration.

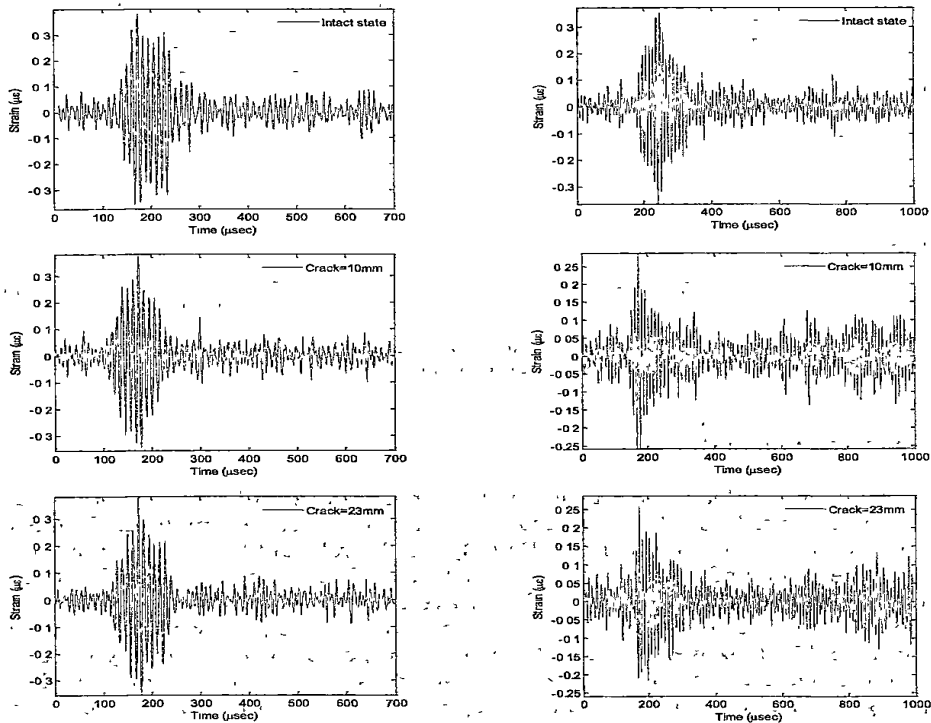


Figure 6. Acquired signals via pitch-catch configuration: (a) left column for excitation frequency at 90 kHz; (b) right column for excitation frequency at 100 kHz.

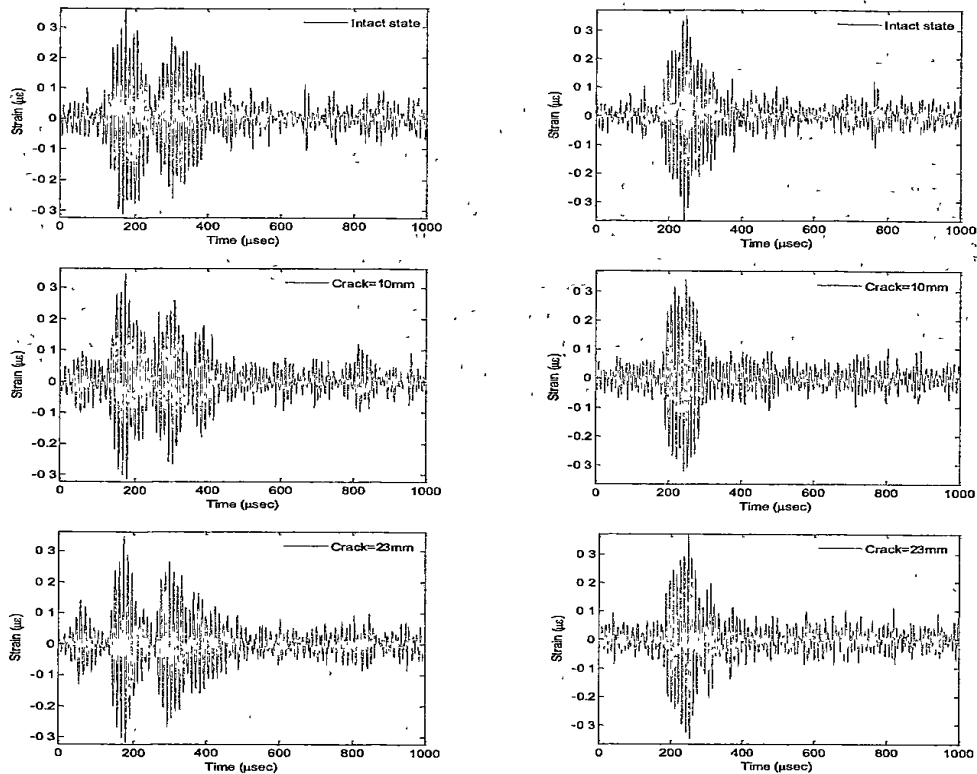


Figure 7. Acquired signals via pulse-echo configuration: (a) left column for excitation frequency at 90 kHz, (b) right column for excitation frequency at 100 kHz.

### Frequency-domain analysis

The procedure for feature extraction and anomaly detection from the guided wave signals is as follows. First, the raw signals were decomposed into multiple frequency regions via discrete wavelet transform (DWT), and the relevant level corresponding to the excited frequency of 62.5-125 kHz was selected, filtering out the signals in other frequency bands. Using a Daubechies wavelet, the raw wave signals were decomposed into five levels corresponding to different frequency regions and the signals in 62.5-125 kHz were extracted. Second, the power spectral density (PSD) of the purified signal is estimated with the use of Welch's method. It splits the signal into overlapping segments, calculates the periodograms of the overlapping segments, and averages the resultant periodograms to yield the PSD. The square roots of PSDs of the purified signals are shown in Figures '8-9. Obvious differences between intact and

damaged conditions of rail can be observed in these spectral curves. Around the center frequency (90 and 100 kHz), the spectral curves of intact rail show higher amplitudes than those of damaged rail. With the increase in crack length, the amplitudes decrease. Although the signals excited by 90 kHz tone bursts exhibit higher amplitudes than those by 100 kHz tone bursts, the latter is found more sensitive to damage. Further, the discrete integration of each PSD is calculated for representing energy, and ratios between the integrals are listed in Table I to quantitatively show differences between damaged and intact situations of the rail.

TABLE I. COMPARISON BETWEEN DAMAGED AND INTACT SITUATIONS

Method	Central frequency	Ratio	Percentage
Pitch-catch	90 kHz	10mm crack/intact:	97.5%
		23mm crack/intact	88.5%
	100 kHz	10mm crack/intact:	76.9%
		23mm crack/intact.	71.2%
Pulse-echo	90 kHz	10mm crack/intact:	77.8%
		23mm crack/intact	70.6%
	100 kHz	10mm crack/intact.	66.9%
		23mm crack/intact:	61.3%

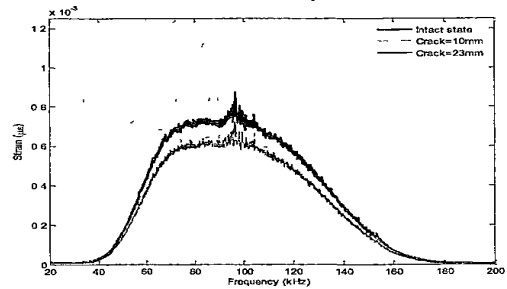
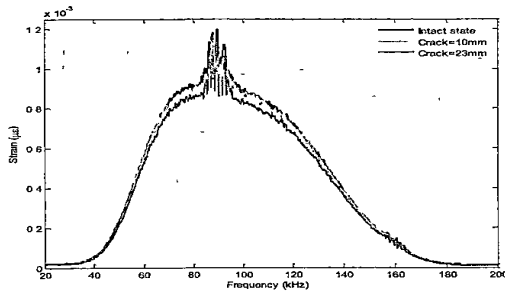


Figure 8 Frequency-domain comparison (pitch-catch configuration). (a) left column for excitation frequency at 90 kHz; and (b) right column for excitation frequency at 100 kHz.

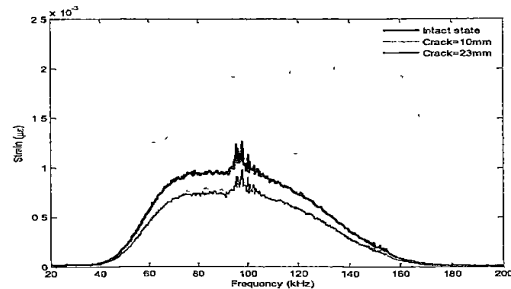
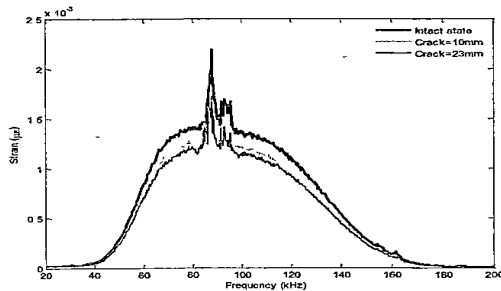


Figure 9 Frequency-domain comparison (pulse-echo configuration). (a) left column for excitation frequency at 90 kHz, and (b) right column for excitation frequency at 100 kHz

## CONCLUSIONS

A fiber optic based ultrasonic guided wave detection system has been developed for rail crack detection, which embraces a controllable tone burst generator, a high-speed interferometric FBG interrogator, and a hybrid PZT-FBG actuating-sensing system. The dispersion characteristic of the rail segment was investigated, by which the excitation frequency and FBG dimension were chosen for appropriate wave generation and response perception. Experimental results showed that the propagation of guided waves in a rail was significantly complicated in both pitch-catch and pulse-echo configurations, and that time-domain signals evidenced insignificant differences between intact and damaged situations of the rail. With the assistance of the wavelet filtering technique, raw signals were purified for accentuating the information of interest. The frequency-domain features of guided waves were extracted from the purified data by using the Welch's power spectral density estimation method. This approach provided better assessment performance than the time-domain analysis in rail crack detection.

## ACKNOWLEDGEMENT

This work is supported by grants from the Innovation and Technology Commission, The Hong Kong SAR Government (Project No.. ITS/343/14) and the Research Institute for Sustainable Urban Development, The Hong Kong Polytechnic University (Project No : 1-ZVCW). The authors would like to express their gratitude to the Hong Kong Branch of National Rail Transit Electrification and Automation Engineering Technology Research Center (1-BBY5), The Hong Kong Polytechnic University. The authors also wish to appreciate the consulting supports from the following optic specialists – Dr. Wai-Shing Man, Amonics Limited, Hong Kong, Ir. Lun-Kai Cheng, TNO, Delft, The Netherlands, and Prof. Xiaoping Dong, Xiamen University, Xiamen, China.

## REFERENCES

1. Clark, R. 2004 "Rail flaw detection overview and needs for future developments," *NDT&E International*, 37(2) 111-118
2. Papaefias, M Ph , C. Roberts, and C L Davis. 2008. "A review on non-destructive evaluation of rails state-of-the-art and future development," *Journal of Rail and Rapid Transit*, 222(4) 367-384
3. Hong, M., Q. Wang, Z. Su, and L. Cheng. 2014 "In situ health monitoring for bogie systems of CRH380 train on Beijing-Shanghai high-speed railway," *Mechanical Systems and Signal Processing*, 45(2). 378-395
4. Rose, J. L , M. J. Avioli, P. Mudge, and R. Sanderson 2004, "Guided wave inspection potential of defects in rail," *NDT&E International*, 37(2) 153-161
5. Loveday, P.W. 2012. "Guided wave inspection and monitoring of railway track," *Journal of Nondestructive Evaluation*, 31(4). 303-309.